

Zn-Doped p-Type Gallium Phosphide Nanowire Photocathodes from a Surfactant-Free Solution Synthesis

Chong Liu,^{†,§} Jianwei Sun,[†] Jinyao Tang,[†] and Peidong Yang^{†,‡,§,*}

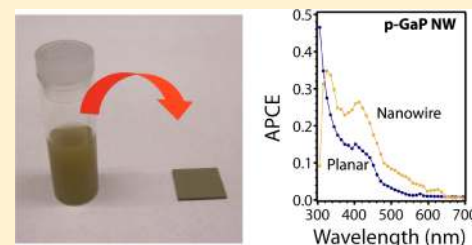
[†]Department of Chemistry, and [‡]Department of Materials Science and Engineering, University of California, Berkeley, California 94720, United States

[§]Materials Sciences Division, Lawrence Berkeley National Laboratory, Berkeley, California 94720, United States

Supporting Information

ABSTRACT: Gallium phosphide (GaP) nanowire photocathodes synthesized using a surfactant-free solution–liquid–solid (SLS) method were investigated for their photoelectrochemical evolution of hydrogen. Zinc as a p-type dopant was introduced into the nanowires during synthesis to optimize the photocathode's response. Investigation of the electrical properties of Zn-doped GaP nanowires confirmed their p-type conductivity. After optimization of the nanowire diameter and Zn doping concentration, higher absorbed photon-to-current efficiency (APCE) over the spectrum was achieved. The versatility of the SLS synthesis and the capability to control the electrical properties suggest that our approach could be generalized to other III–V and II–VI semiconductors.

KEYWORDS: Gallium phosphide, nanowire, photoelectrochemistry, surfactant-free solution synthesis



Since the first report of photoassisted water-splitting in 1972,¹ producing fuels from solar energy has been an attractive application of semiconductor photoelectrodes.^{2–5} By converting solar energy into chemical fuels, the energy harvested from the sun can be efficiently stored, transported, and used. Theoretically, for a single-band gap system this approach could reach an efficiency up to 17% (assuming a 0.8 V overpotential).⁶ Moreover, when two semiconductors are coupled as a photoanode and photocathode to mimic natural photosynthesis,^{7–9} an even higher theoretical efficiency has been predicted.⁶

Compared to other available semiconductors, gallium phosphide (GaP) is considered a highly promising photocathode material for solar-fuel conversion.^{7,8,10} Its large photovoltage enables it to be coupled with photoanode materials for complete water-splitting under zero external bias, and its high conduction band edge (−0.6 V versus NHE at pH = 0)⁵ allows it to reduce not only water into hydrogen (0 V versus NHE)^{11–14} but also CO₂ into chemical fuels (−0.17 V versus NHE to generate CH₄)^{15,16} with incident photon-to-current efficiency (IPCE) up to 30% at 400 nm;¹⁴ however, the conventional planar geometry from a single-crystalline wafer is not ideal for inexpensive or large-scale processing. It also poses an obstacle to exploring the potential of GaP fully, since in the planar geometry most of the photons absorbed by GaP^{13,14,17,18} do not fall within the charge collection layer, as is required for an efficient photoelectrode.⁴

Recent progress indicates that this issue could be solved when the photoelectrode is composed of semiconductor micro- or nanowires.^{19–23} Compared to a planar electrode, the larger surface area and relative band-bending volume of a wire geometry not only allows more efficient charge separation but

also reduces the current density and therefore the overpotential at the surface.^{24,25} These advantages, properly applied to GaP, could lead to higher charge separation efficiency.

In general, there are three major requirements for practical and large-scale fabrication of nanowire photoelectrodes. First, the synthesis of the material should be scalable and inexpensive. This condition implies that for GaP, solution-phase synthesis²⁶ is potentially preferred to gas-phase synthesis²⁷ because of the small yield of the latter approach. Second, the surface of the nanowires should be free of insulating organics that hinder charge transfer across the semiconductor–electrolyte interface, so conventional solution synthesis that often requires surfactants/ligands^{28,29} is not desirable. Finally, the electrical properties of the synthesized nanowires should be tunable. The advantages of nanowire photoelectrodes will diminish unless their diameter, doping level, and minority carrier diffusion length can be systematically controlled.^{24,30} Although doped semiconductor nanocrystals³¹ and nanowires^{32,33} from solution-phase synthesis have been reported, there have been no studies that correlate the electrical properties of solution-grown nanowires to their photoelectrochemical performance.

In this report, the electrical properties of GaP nanowires were modified by in situ Zn doping during their synthesis, which was based on the surfactant-free solution–liquid–solid (SLS) synthetic method developed before,^{34–36} p-type GaP nanowires of various doping levels were obtained. At the optimized conditions, the nanowire photoelectrode provides photocurrent up to 85% to that of a single crystalline GaP

Received: August 2, 2012

Revised: September 19, 2012

Published: October 1, 2012

wafer, along with higher absorbed photon-to-current efficiency (APCE) performance over the whole spectrum. This approach could also be applied to other semiconductor materials for the fabrication of large-scale photoelectrodes with high surface area.

The surfactant-free synthesis of GaP nanowires has been reported in our previous paper.³⁶ The nanowires' growth follows a self-seeded SLS mechanism³⁵ in which Ga metal nanodroplets are first generated and then function as catalytic sites for further growth. Prolonged stirring after injection of the precursor helps the Ga nanodroplets merge with each other before the growth of the GaP nanowire takes place, therefore allowing control of the diameter of the nanowires (Supporting Information Figure 1). After growth, removal of the Ga nanodroplets by hydrochloric acid yields clean GaP nanowires.

To optimize the electrical properties of the GaP nanowires, a p-type shallow dopant, typically Zn,³⁷ is necessary to control the acceptor concentration. Diethylzinc (DEZn) was added as the source of Zn³⁸ during the synthesis. Because of the weaker Zn–C bond strength (35 kJ/mol) as compared to that of the Ga–C bond (59 kJ/mol),³⁸ most of the DEZn decomposes into metallic zinc during formation of the metal droplets, yielding Ga–Zn alloy droplets that can catalyze the growth of the GaP nanowires. Inductively coupled plasma-atomic emission spectrometry (ICP-AES) was applied to determine the elemental composition of the resultant nanowires. Despite the fast decomposition of DEZn, only 5–10% of the zinc precursor added to the reaction was introduced into the GaP lattice during growth (Table 1). The Zn doping of GaP

images show that the nanowires' morphology remains the same upon Zn-doping (Figure 1a,c, Supporting Information Figure

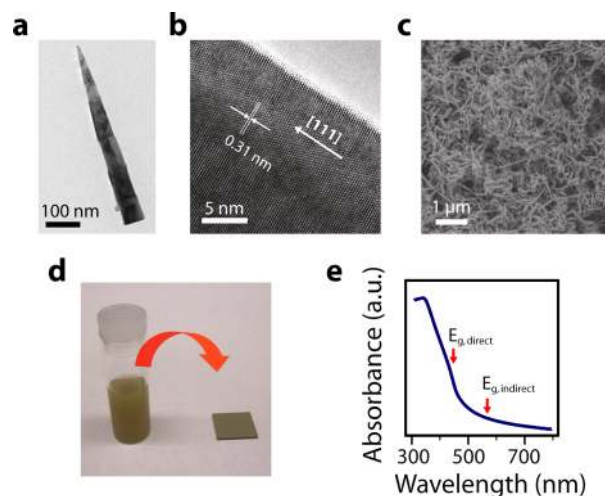


Figure 1. Structural and optical properties of Zn-doped GaP nanowires (0.19 atom % Zn versus Ga). (a) TEM image of a Zn-doped GaP nanowire after the removal of Ga droplets. (b) HRTEM image indicates that the nanowire is single-crystalline and grows along the $\langle 111 \rangle$ direction. (c) SEM image of the same nanowires when prepared as a photoelectrode by drop casting ($64 \mu\text{g}/\text{cm}^2$). (d) Photograph of the GaP nanowire dispersion and GaP photoelectrode. (e) UV-vis absorption spectrum of GaP nanowires dispersed in acetone. The positions of the direct ($E_{g,\text{direct}}$) and indirect ($E_{g,\text{indirect}}$) band gaps of bulk GaP are shown. The absorption tail in longer wavelengths is due to the strong scattering of the nanowires.

Table 1. Photoelectrochemical Performance of GaP Nanowire Photoelectrodes

DEZn/ TEGa (%) ^a	D (nm) ^b	Zn atom % ^c	N_A (cm^{-3}) ^d	d (nm) ^e	j_{ph} ($\mu\text{A}/\text{cm}^2$) ^f	$V_{\text{oc,ph}}$ (mV) ^g	η ^h (%)
0	25 ± 5			35	11	145	75
0	89 ± 24			35	23	195	81
1	90 ± 27	0.19	4×10^{19}	11	29	220	
5	86 ± 22	0.57	1×10^{20}	3.5	33	280	
10	93 ± 33	0.98	2×10^{20}	2.4	61	247	79
15	91 ± 29	1.3	3×10^{20}	2.0	43	226	
20	87 ± 27	1.6	4×10^{20}	1.8	25	141	

^aThe molar ratio between DEZn and TEGa precursors in the SLS synthesis. ^bAverage diameter of the GaP nanowires. ^cAtomic concentration of Zn dopant versus Ga, measured by ICP-AES. ^dAcceptor concentration of zinc calculated from ICP-AES measurement. ^eDepletion width of GaP nanowires at different acceptor concentration, calculated assuming an abrupt planar Schottky junction with 0.5 V band-bending. ^fPhotocurrent of nanowire photocathodes in pH 5.2 buffer at 0.1 V versus RHE, under simulated one-sun conditions (AM1.5G). ^gOpen-circuit photovoltage of GaP nanowire photocathodes in the same conditions as for the photocurrent measurements. ^hFaradic efficiency of hydrogen evolution, measured by gas chromatography.

nanowires may occur from the Ga–Zn alloy droplets in a process similar to the incorporation of Al from metal droplets during GaAs growth, which results in $\text{Al}_x\text{Ga}_{1-x}\text{As}$ nanowires.³⁹ The concentration of Zn in GaP nanowires could be quantitatively controlled up to 2 atomic percent (atom %) versus Ga by changing the amount of DEZn (Table 1), while the nanowire geometry and optical absorption features of gallium phosphide were retained. Transmission electron microscope (TEM) and scanning electron microscope (SEM)

1), and high-resolution TEM (HRTEM) images (Figure 1b) reveal that the GaP lattice grows along the $\langle 111 \rangle$ direction with lattice spacing of 0.31 nm.³⁶ The UV-vis absorption spectrum of a suspension of Zn-doped nanowires (Figure 1e) is the same as that of the undoped nanowires,³⁶ implying that introducing Zn does not alter the band gap of GaP.¹⁷

Several approaches were used to demonstrate the p-type behavior of the Zn-doped GaP nanowires (Table 1). Single-nanowire field effect transistors (FET) were constructed to determine the carrier type and concentration (Figure 2a). For a 0.19 atom % Zn-doped GaP nanowire (Figure 2b), the negative transconductance (I_{DS}/V_g) was measured to be $-4.5 \text{ nA}/\text{mV}$ at $V_{\text{DS}} = 1 \text{ V}$, which corresponds to an acceptor concentration of $1 \times 10^{19} \text{ cm}^{-3}$. This measured acceptor concentration corresponds well with the 0.19 atom % zinc concentration (equivalent to $4 \times 10^{19} \text{ cm}^{-3}$) from elemental analysis, implying that the included Zn does contribute to p-type behavior of the GaP nanowires. In addition, open-circuit photovoltage and Mott–Schottky measurements were performed to test the band bending at the semiconductor-electrolyte interface (Figure 2c,d). Larger open-circuit photovoltage (up to 280 mV) was found for Zn-doped GaP nanowires (Table 1), indicating that the increased acceptor concentration prevents full depletion of the nanowire and allows a barrier of greater height to form at the semiconductor-electrolyte interface. Besides the p-type behavior, the Mott–Schottky measurement gives the flat-band potential of GaP nanowires at around 0.52 V versus the reversible hydrogen electrode (RHE), which is consistent with the literature on planar substrates.^{5,16} Overall, the photovoltage and Mott–Schottky measurements demonstrate that these Zn-doped GaP

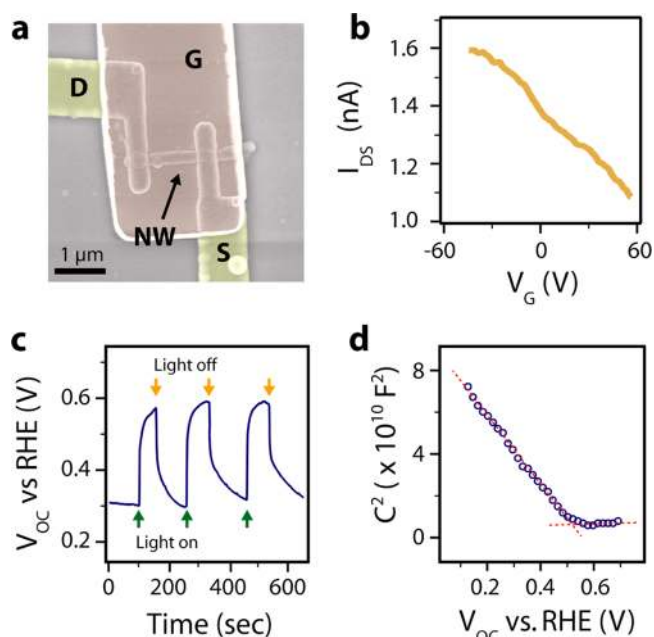


Figure 2. Electrical properties of Zn-doped GaP nanowires (0.19 atom % Zn versus Ga). (a) SEM image of a single-nanowire FET device. The source (S) and drain (D) are colored in yellow, and the top gate (G) is colored in pink. (b) Plot of the current within the nanowire channel (I_{DS}) versus the gate voltage (V_G), indicating p-type conductivity ($V_{DS} = 1$ V). (c) Open-circuit photovoltage measurements of the nanowire photoelectrode in pH 5.2 buffer under simulated one-sun conditions (AM1.5G). (d) Mott–Schottky measurement of a nanowire photoelectrode in pH 5.2 buffer. The intercept of the dashed line indicates the flat-band potential of the GaP nanowires.

nanowires possess desirable band bending at the semiconductor–electrolyte interface to act as a photocathode for hydrogen evolution.

To test the photoelectrochemical performance of the doped GaP nanowires, a solution of nanowires was drop cast onto a conductive substrate. After annealing to improve the electrical contact between the substrate and the nanowires, a uniform electrode was obtained (Figure 1c,d). The volume of the nanowire dispersion applied during drop casting controls the thickness of the nanowire film. Typical loading amount was about $60 \mu\text{g}/\text{cm}^2$, which is about 1/3000 of the amount of material used in a planar wafer electrode ($0.2 \text{ g}/\text{cm}^2$). After preparation, the nanowire electrodes were tested in pH 5.2 buffer solutions under chopped, one-sun illumination (AM1.5G) using a conventional three-electrode configuration (Figure 3a, Table 1). For comparison, the performance of a single crystalline p-type GaP wafer was also examined under the same conditions. The planar p-type GaP electrode exhibits comparable photocurrent density with other reports.^{14,16} All nanowire electrodes showed onset potentials at about 0.5 V versus RHE, consistent with the flat-band potential from the Mott–Schottky experiment (Figure 2d). Compared to other recently studied photocathode materials (for example, silicon²⁰), this relatively anodic onset potential (0.5 V versus RHE) is advantageous, potentially allowing GaP to couple with a wider selection of photoanode materials to realize complete water splitting using two semiconductors photoelectrodes. Another noticeable feature is that the nanowire electrode shows much smaller transient photocurrent than the planar electrode (Figure 3a). Since the transient photocurrent arises from photogenerated carriers that accumulate at the semiconductor–electrolyte interface because of slow reaction kinetics or surface state traps,⁴⁰ the nanowire electrode’s small transient current suggests that its large surface area reduces its current density and required overpotential.

A systematic study was performed to investigate factors affecting the photoelectrochemical properties of the nanowires. Although all GaP nanowires studied generated cathodic photocurrent, larger diameter wires corresponded to larger photovoltages and higher photocurrent densities (Table 1). When keeping the diameter of the nanowires constant and

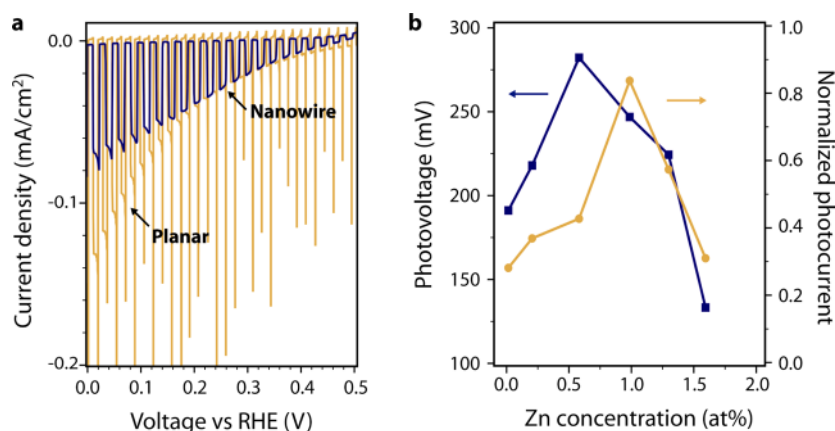
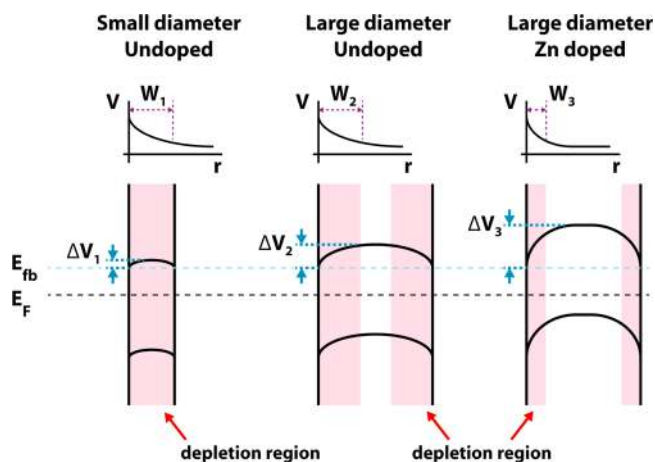


Figure 3. Photoelectrochemical performance of the GaP photocathode in pH 5.2 buffer. (a) I – V scans of GaP nanowire (blue) and planar (yellow) photocathodes under chopped illumination. The illumination is simulated one-sun conditions (AM1.5G). The nanowire electrode is made of 0.98 atom % Zn-doped GaP nanowire with loading amount of $64 \mu\text{g}/\text{cm}^2$. When close to 0 V versus RHE, the planar electrode yields higher photocurrent density, mostly because of its greater thickness and increased depletion layer; however, it should be noted that the performance at more anodic regions (larger than 0.2 V versus RHE) is of greater importance because only in this region can the GaP photocathode be coupled with a photoanode to realize a complete water-splitting reaction without external bias.^{7,8} (b) The correlation of photovoltage (blue) and photocurrent (yellow) with the concentration of Zn dopant in GaP nanowires. The photocurrent data was measured at 0.1 V versus RHE and normalized with the photocurrent of planar GaP electrode at the same bias. The photovoltage is measured as the difference of open-circuit potential between dark and simulated one sun illumination (AM1.5G).

increasing the doping concentration of Zn, an optimal doping level (0.6~1 atom %) was achieved for the photoactivity of the GaP nanowires with average diameter of 90 nm (Figure 3b). For undoped nanowires of about 25 nm diameter, the relatively large depletion region width (~ 30 nm, calculated as planar abrupt junction with 0.5 V barrier height) from low doping level (at most 10^{18} cm^{-3} based on FET data) leads to complete depletion within the semiconductor. This depletion yields low photovoltage and photocurrent because of the reduced band bending at the semiconductor–electrolyte interface and the large ohmic resistance along the length of the wire (Scheme 1).^{24,30} Larger diameter nanowires (~ 90 nm) alleviate this

Scheme 1. Schematic Illustration of the Electrostatics of a GaP Nanowire in Electrolyte with Varying Diameters and Doping Levels^a



^a W is the width of band-bending or depletion at the semiconductor–electrolyte interface, ΔV is the band-bending between the nanowire core and the interface, E_{fb} is the flat-band potential of GaP, and E_F is the Fermi level of the system. The nanowire of small diameter suffers small band-bending. Large diameter alleviates this issue; however, it was not completely solved until Zn was introduced.

issue, but the depletion width is still too large until extra Zn dopant is introduced to increase the acceptor concentration and reduce the depletion region width (~ 10 nm for 10^{19} cm^{-3}). Zn doping prevents the complete depletion of the nanowire, leading to a larger photovoltage (Scheme 1). Additionally, a narrower band-bending region means a stronger electric field close to the semiconductor–electrolyte interface, yielding higher charge separation efficiency and photocurrent density.³⁰ On the other hand, the introduction of dopants also increases recombination within nanowire, meaning that an excessively high Zn concentration would be detrimental for efficient charge separation. This trade-off leads to an optimal Zn concentration for the best photocathode performance, as observed in our current study (Figure 3b).

When the properties of GaP nanowires were optimized, the photocurrent density of Zn-doped GaP nanowires was about 85% to that of the single crystalline wafer at 0.1 V versus RHE (Figure 3a). In addition, 80% Faradic efficiency of H_2 evolution was observed, affirming that most of the photocurrent contributes to reduce protons (Table 1). Because a comparable photocurrent density was achieved while using much less material, these results demonstrate that solution-synthesized surfactant-free Zn-doped GaP nanowires are a promising photocathode material for water splitting.

Even though its photocurrent is only comparable to that exhibited by a planar GaP electrode (Figure 3a, Supporting Information Figure 2), the GaP nanowire photocathode has much higher charge separation efficiency, as could be seen from the APCE spectrum (Figure 4a). Closer examination of the

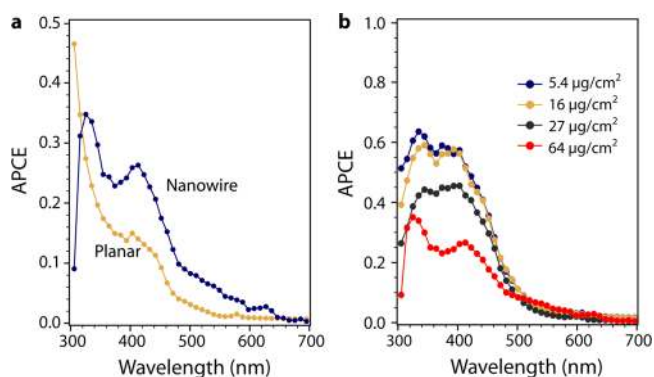


Figure 4. (a) Comparison of the absorbed photon-to-current efficiency (APCE) spectra between GaP planar (blue) and nanowire (yellow) photocathodes of $64 \mu\text{g}/\text{cm}^2$ loading amount. (b) APCE spectra of GaP nanowire photocathodes at different loading amounts. In both figures, the GaP nanowires were doped with 0.98 atom % Zn versus Ga, and the spectra were measured at 0.1 V versus RHE under simulated one-sun conditions (AM1.5G).

APCE spectrum of the nanowire photoelectrodes with different loading amounts shows that the APCE increases with reduced loading amount (Figure 4b) and reaches a maximum with less than a monolayer of GaP nanowires (Supporting Information Figure 3). This result indicates that charge transport to the electrode from nanowires lacking direct contact with the underlying substrate is difficult because of the semi-insulating native oxide at the GaP surface.⁴¹ By removing the necessity of charge transport through the nanowire/nanowire interface, the submonolayer of Zn-doped GaP nanowires reaches 57% efficiency at 400 nm (0.1 V versus RHE) (Figure 4b). By improving the contact between wires, the overall photocurrent of the GaP nanowire films could be further improved.

Semiconductor nanowire photoelectrodes have the potential to be scaled up for practical conversion of solar energy to fuels. Gallium phosphide, a very promising material for both hydrogen evolution and CO_2 reduction,^{4,5} has been tested as one example. On the basis of the requirements of scalability and a clean semiconductor–electrolyte interface, GaP nanowires of different diameters were synthesized by a surfactant-free solution approach via the SLS mechanism.³⁶ The electrical properties of these nanowires were engineered by introducing p-type Zn dopant during the synthesis. Using only 1/3000 of the amount of GaP in a single crystalline wafer and a scalable drop-casting process for electrode preparation, the photo-current density of the Zn-doped GaP nanowires was comparable to that of a single crystalline wafer, with higher APCE value over the spectrum. These findings not only demonstrate the advantage of nanowire electrodes but also enrich our understanding of nanowire photoelectrochemistry. The versatility of the SLS synthesis,³⁵ and the capability to control the electrical properties by introducing dopants during synthesis,³⁸ suggest that our approach could be generalized to other III–V and II–VI semiconductors, and ultimately coupled with a photoanode to realize a complete solar-to-fuel reaction.

■ ASSOCIATED CONTENT

Supporting Information

The Supporting Information includes the experimental details, TEM images of GaP nanowires of controlled diameters, IPCE and APCE data, and a SEM image of submonolayer of GaP nanowire photoelectrodes. This material is available free of charge via the Internet at <http://pubs.acs.org>.

■ AUTHOR INFORMATION

Corresponding Author

*E-mail: p_yang@berkeley.edu.

Notes

The authors declare no competing financial interest.

■ ACKNOWLEDGMENTS

We thank S. Brittman for helpful discussion. This work was supported by the Director, Office of Science, Office of Basic Energy Sciences, Materials Sciences and Engineering Division, of the U.S. Department of Energy under Contract No. DE-AC02-05CH11231.

■ REFERENCES

- (1) Fujishima, A.; Honda, K. *Nature* **1972**, *238*, 37.
- (2) Bard, A. J.; Fox, M. A. *Acc. Chem. Res.* **1995**, *28*, 141.
- (3) Lewis, N. S.; Nocera, D. G. *Proc. Natl. Acad. Sci. U.S.A.* **2006**, *103*, 15729.
- (4) Walter, M. G.; Warren, E. L.; McKone, J. R.; Boettcher, S. W.; Mi, Q.; Santori, E. A.; Lewis, N. S. *Chem. Rev.* **2010**, *110*, 6446.
- (5) Grätzel, M. *Nature* **2001**, *414*, 338.
- (6) Bolton, J. R.; Strickler, S. J.; Connolly, J. S. *Nature* **1985**, *316*, 495.
- (7) Ohashi, K.; Mccann, J.; Bockris, J. O. M. *Nature* **1977**, *266*, 610.
- (8) Nozik, A. J. *Appl. Phys. Lett.* **1976**, *29*, 150.
- (9) Kudo, A. *MRS Bull.* **2011**, *36*, 32.
- (10) Mettee, H.; Otvos, J. W.; Calvin, M. *Sol. Energy Mater.* **1983**, *4*, 443.
- (11) Tomkiewicz, M.; Woodall, J. M. *Science* **1977**, *196*, 990.
- (12) Butler, M. A.; Ginley, D. S. *J. Electrochem. Soc.* **1980**, *127*, 1273.
- (13) Li, J.; Peat, R.; Peter, L. M. *J. Electroanal. Chem. Interfacial Electrochem.* **1984**, *165*, 41.
- (14) Hagedorn, K.; Collins, S.; Maldonado, S. *J. Electrochem. Soc.* **2010**, *157*, D588.
- (15) Halmann, M. *Nature* **1978**, *275*, 115.
- (16) Barton, E. E.; Rampulla, D. M.; Bocarsly, A. B. *J. Am. Chem. Soc.* **2008**, *130*, 6342.
- (17) Aspnes, D. E.; Studna, A. A. *Phys. Rev. B* **1983**, *27*, 985.
- (18) Smith, B. L.; Abbott, M. *Solid-State Electron.* **1972**, *15*, 361.
- (19) Boettcher, S. W.; Spurgeon, J. M.; Putnam, M. C.; Warren, E. L.; Turner-Evans, D. B.; Kelzenberg, M. D.; Maiolo, J. R.; Atwater, H. A.; Lewis, N. S. *Science* **2010**, *327*, 185.
- (20) Boettcher, S. W.; Warren, E. L.; Putnam, M. C.; Santori, E. A.; Turner-Evans, D.; Kelzenberg, M. D.; Walter, M. G.; McKone, J. R.; Brunschwig, B. S.; Atwater, H. A.; Lewis, N. S. *J. Am. Chem. Soc.* **2011**, *133*, 1216.
- (21) Hwang, Y. J.; Boukai, A.; Yang, P. *Nano Lett.* **2008**, *9*, 410.
- (22) Lin, Y.; Zhou, S.; Sheehan, S. W.; Wang, D. *J. Am. Chem. Soc.* **2011**, *133*, 2398.
- (23) Cho, I. S.; Chen, Z.; Forman, A. J.; Kim, D. R.; Rao, P. M.; Jaramillo, T. F.; Zheng, X. *Nano Lett.* **2011**, *11*, 4978.
- (24) Foley, J. M.; Price, M. J.; Feldblyum, J. I.; Maldonado, S. *Energy Environ. Sci.* **2012**, *5*, 5203.
- (25) Hochbaum, A. I.; Yang, P. *Chem. Rev.* **2009**, *110*, 527.
- (26) Park, J.; An, K.; Hwang, Y.; Park, J.-G.; Noh, H.-J.; Kim, J.-Y.; Park, J.-H.; Hwang, N.-M.; Hyeon, T. *Nat. Mater.* **2004**, *3*, 891.
- (27) Duan, X.; Lieber, C. M. *Adv. Mater.* **2000**, *12*, 298.
- (28) Yin, Y.; Allivisatos, A. P. *Nature* **2005**, *437*, 664.
- (29) Liu, Z.; Sun, K.; Jian, W.-B.; Xu, D.; Lin, Y.-F.; Fang, J. *Chem.—Eur. J.* **2009**, *15*, 4546.
- (30) Hagedorn, K.; Forgacs, C.; Collins, S.; Maldonado, S. *J. Phys. Chem. C* **2010**, *114*, 12010.
- (31) Erwin, S. C.; Zu, L.; Haftel, M. I.; Efros, A. L.; Kennedy, T. A.; Norris, D. J. *Nature* **2005**, *436*, 91.
- (32) Yuhas, B. D.; Zitoun, D. O.; Pauzauskie, P. J.; He, R.; Yang, P. *Angew. Chem., Int. Ed.* **2006**, *45*, 420.
- (33) Li, Z.; Cheng, L.; Sun, Q.; Zhu, Z.; Riley, M. J.; Aljada, M.; Cheng, Z.; Wang, X.; Hanson, G. R.; Qiao, S.; Smith, S. C.; Lu, G. Q. *Angew. Chem., Int. Ed.* **2010**, *122*, 2837–2841.
- (34) Trentler, T. J.; Hickman, K. M.; Goel, S. C.; Viano, A. M.; Gibbons, P. C.; Buhro, W. E. *Science* **1995**, *270*, 1791.
- (35) Wang, F.; Dong, A.; Sun, J.; Tang, R.; Yu, H.; Buhro, W. E. *Inorg. Chem.* **2006**, *45*, 7511.
- (36) Sun, J.; Liu, C.; Yang, P. *J. Am. Chem. Soc.* **2011**, *133*, 19306.
- (37) Swaminathan, V.; Macrander, A. T. *Materials Aspects of GaAs and InP Based Structures*; Prentice-Hall, Inc.: New York, 1991.
- (38) Stringfellow, G. B. *Organometallic Vapor-Phase Epitaxy, Theory and Practice*; Academic Press, Inc.: San Diego, CA, 1989.
- (39) Markowitz, P. D.; Zach, M. P.; Gibbons, P. C.; Penner, R. M.; Buhro, W. E. *J. Am. Chem. Soc.* **2001**, *123*, 4502.
- (40) Le Formal, F.; Tetreault, N.; Cornuz, M.; Moehl, T.; Grätzel, M.; Sivula, K. *Chem. Sci.* **2011**, *2*, 737.
- (41) Iwasaki, H.; Mozokawa, Y.; Nishitani, R.; Nakamura, S. *Jpn. J. Appl. Phys.* **1978**, *17*, 1925.